Available online at www.sciencedirect.com
ScienceDirect
Polymer 47 (2006) 8183–8193
polymer
www.elsevier.com/locate/polymer

Control of optical anisotropy at large deformations in PMMA/chlorinated-PHB (PHB-Cl) blends: Mechano-optical behavior

Baris Yalcin [a], Mukerrem Cakmak [a,*], Ali Hakan Arkın [b], Baki Hazer [b], Burak Erman [c]

[a] *Department of Polymer Engineering, University of Akron, Akron, OH 44325-0301, United States*
[b] *Zonguldak Karaelmas University, Zonguldak 67100, Turkey*
[c] *Koc University, Istanbul, Turkey*

Received 2 August 2006; received in revised form 21 September 2006; accepted 24 September 2006
Available online 16 October 2006

Abstract

There is a continuing need to produce polymer films with high optical clarity with ability to dial in the optical properties including refractive indices and optical anisotropies. In this research, we investigated the mechano-optical behavior of PMMA/PHB-Cl blend films during uniaxial deformation and mapped out the composition-birefringence-processing relationships. The results indicate the presence of a broad glass transition for the composition range investigated that indicates the development of micro-heterogeneities particularly at the higher concentration of PHB-Cl. However, this did not detrimentally influence the optical transparency of the solvent cast films as the size of these micro-heterogeneities remains well below the size range to affect the transparency. Optical retardation behavior of the films can be altered from negative to positive by increasing the PHB-Cl concentration from 0 to 20 wt%. The films with 18 wt% PHB-Cl are predicted to exhibit zero birefringence even when they are stretched to large deformations. This dialability of optical properties makes these materials suitable for optical device applications such as CD and DVDs as well as optical retarder films for liquid-crystal display applications.
© 2006 Elsevier Ltd. All rights reserved.

Keywords: Polymethylmethacrylate (PMMA); Microbial polyester poly(3-hydroxybutyrate) (PHB); Birefringence

1. Introduction

Bacteria synthesized poly hydroxyl alkanoates and their copolymers have been gaining wider interest particularly from the food packaging industry for their biodegradability. PHAs are synthesized by prokaryotic organisms and stored in their cytoplasm [1]. Various types of PHAs with diverse physical properties have been produced using alkanols, alkanoic acids, edible oily acids, and bromo derivatives of alkanoic acids [2–9]. The general structure of the repeating unit of these polyesters is shown below, in which R varies depending on the type of bacteria and the feed. It is typically $-(CH_2)_n-CH_3$ for most naturally occurring PHAs.

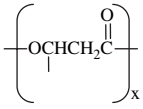

The physical properties of these PHAs vary widely from crystalline-brittle to soft-sticky as the length of the side chain on β-carbon increases. PHB (R: CH_3), though highly crystalline, has narrow processing window and tends to be brittle in unmodified form. It possesses T_m of 175 °C and a T_g of 0–4 °C. It is unstable in the melt [10] and the thermal degradation begins around its melting point. PHB degrades to crotonic acid at high temperatures which leads to a decrease in molecular weight and hence serious processing problems [11]. Particularly for film applications, it has low elongational extensibility which is a major disadvantage. For these reasons, attempts were made to improve its mechanical properties and processibility either by the modification of PHB molecular

* Corresponding author.
E-mail address: cakmak1@uakron.edu (M. Cakmak).

0032-3861/$ - see front matter © 2006 Elsevier Ltd. All rights reserved.
doi:10.1016/j.polymer.2006.09.051

structure itself through copolymerization [1,12–14] or blending it with other commercial synthetic polymers [15–24] or additives like plasticizers [25], lubricants and nucleation agents. Currently, the blending route appears more promising than the copolymerization route to enhance the performance of these materials. In particular, copolymerization route is generally more expensive and properties of these tend not to be attractive.

A synergistic blend of PHB with any other commercial synthetic polymer should display improved properties, lower the cost of production and most importantly be biodegradable.

PMMA is particularly important for blending with PHB because it is a biocompatible polymer that allows the polyester to be used in bio applications. As for optics and photonics applications, PMMA is one of the key materials used in a variety of optical devices such as polymer optical fibers, optical films for liquid-crystal displays, optical disks, lenses, etc. because of its exceptional clarity in the visible range. Optical polymers that exhibit intrinsic zero birefringence are desirable to minimize the distortion of light passage through them for optical devices such as DVDs and CDs made by injection molding, where the polymer chains are subjected to high orientation fields. In other applications, low retardation films are needed for optical retarders used in the construction of liquid-crystal displays through film stretching processes.

When PMMA is oriented at temperatures below or near its T_g, it exhibits negative birefringence in the order of 10^{-4}. The negative birefringence in oriented PMMA is attributed to the ester side groups which render high polarizability in the direction transverse to the chain axis [26–29]. The conformation and the motion of the ester side groups in PMMA influence the measured birefringence levels significantly. Exposing pre-oriented PMMA samples of different stereo forms to a range of temperatures from $-200\,^{\circ}C$ up to their corresponding T_g, Andrews and Hammack observed that the birefringence levels could be reversed instantly with temperature [26]. Although this instant reversible nature of birefringence was first attributed to the thermally induced rotation of the ester side groups and considered to be a thermal equilibrium value, the same authors later on suggested that the dipole associations between the ester side groups played an important role in the temperature dependence of birefringence [29]. In spite of the uncertainty associated with the explanation, these studies show the importance of the ester side groups in birefringence development in PMMA. In polymers such as PE, PP or PET, the polarizability associated with the side groups is very low and hence their contribution to the measured birefringence is insignificant. With such polymers, one is not concerned as to what happens to the side chains, i.e. conformation or orientation, during processing. However, for polymers where the polarizability anisotropy is predominantly associated with the side groups, such as phenyl for PS or ester for PMMA, one should pay attention to the orientation of the side groups and processes that influence them. The maximum negative attainable birefringence in stretched PMMA was calculated to be -43×10^{-4} and -35.5×10^{-4} based on broadline NMR [30] and laser Raman spectroscopy [31] measurements.

In order to obtain products exhibiting zero birefringence, PMMA is usually blended with other polymers that exhibit positive birefringence at these temperatures. These polymers include PVC [32,33], PVDF [34] and PEO [35]. Another requirement for use in optical devices is that the blends should exhibit high transparency. When phase separation between the two polymers occurs, transparency can be lost through scattering. Therefore, an alternate route to synthesize zero-birefringence polymers, i.e. random copolymerization of the positive and negative birefringence monomers was proposed and demonstrated [36,37]. Another method of synthesizing zero-birefringence polymers, i.e. anisotropic molecule doping method, was also reported in which the rod-like molecules with polarizability anisotropy are introduced to compensate for the orientational birefringence [38,39]. Compensation of the birefringence by a birefringent crystal has also been reported [40].

Regardless of the synthesis methods described above, current optical polymer materials that are derived from petrochemicals (polycarbonate, PMMA) are problematic when it comes to disposal, especially when they are used to create optical storage media, i.e. CDs and DVDs. Recently, Sanyo Electric Co Ltd. and Japan's Mitsui Chemicals Inc. have announced their first biodegradable optical discs based on poly(lactic acid) (PLA) derived from corn.

In the light of these recent advances in the area, our motivation in this paper is to tailor the use of PMMA in combination with chlorine functionalized PHB (PHB-Cl) to obtain polymers exhibiting low or zero in-plane film birefringence. In order to assess their suitability for these optical applications, we have investigated real time optical (birefringence) and mechanical properties of chlorinated PHB-Cl/PMMA blends in uniaxial deformation mode at elevated temperatures where they are typically processed in commercial processing operations.

2. Experimental

2.1. Materials

All the chemicals necessary for the synthesis of chlorinated PHBs were purchased from Aldrich. Chloroform ($CHCl_3$), carbon tetrachloride (CCl_4), methanol (MeOH), hydrogen chloride (HCl), sulfuric acid (H_2SO_4) and potassium permanganate ($KMnO_4$) were used as received.

2.1.1. Synthesis of chlorinated poly(3-hydroxybutyrate) (PHB-Cl)

Alcaligenes eutrophus (Deutsche Sammlung von Microorganismen und zell kulturen GmbH, DSM # 428) was grown on glucose in a 10 L fermenter at 30 °C in E-2 medium, and the resulting PHB polymer was extracted in a conventional manner according to the procedures cited in the literature [41,42]. Molecular weight (M_n) and polydispersity index (PDI) of PHB were 9.7×10^4 and 4.6, respectively.

PHB was chlorine functionalized according to our previous procedure reported elsewhere [43,44]. Excess HCl was added dropwise to the $KMnO_4$ crystals placed in a two-necked round-bottomed flask in order to produce chlorine gas (1 g

of chlorine gas needs 0.89 g of $KMnO_4$). Required moles of the produced gas were passed, at a bubble per second, through the concentrated H_2SO_4, an empty wash bottle, and then a solution of PHB in $CHCl_3/CCl_4$ (80/20 v/v) in an ice bath under sunlight. The PHB-Cl solution was left in a refrigerator overnight. The solvent was evaporated, and the crude polymer was washed with MeOH, dried under vacuum, and then fractionally precipitated. Fractional precipitation was performed by dropwise addition of MeOH to a 5 mL stirring solution of crude PHB in $CHCl_3$ until completion of the first precipitation. After decantation, the upper solvent was followed by the addition of MeOH until no more precipitation. The precipitated polymer fractions were dried under vacuum.

2.1.2. Preparation of PHB-Cl and PMMA blends

Appropriate amounts of PHB-Cl and PMMA polymers were dissolved and mixed in $CHCl_3$ solution until clear solution was obtained. The polymer sheets were cast from this solution at a thickness of 0.3 and 0.5 mm. The solvent was removed at room temperature in a two-step procedure. First, the solution was kept under ambient atmosphere for 2 days. After 2 days, vacuum was applied for another 2 days to ensure complete solvent removal. Blends were prepared at a ratio of 0/100, 10/90 and 20/80 (wt/wt).

2.2. Thermal analysis

Differential scanning calorimeter (DSC-TA instrument) was used for the thermal analysis of the blends. Polymer (10 mg) was cut from solvent cast sheets and crimped into hermetic aluminum pans. The samples were heated from −100 to +160 °C in a nitrogen atmosphere at a rate of 10 °C/min, quenched and heated second time using the same range and heating rate. This ensured the removal of any solvent present in the samples due to solution casting.

2.3. Mechano-optical properties

Dumbbell-shaped samples were cut from cast sheets to a width of 25 mm and a length of 30 mm. The samples were stretched in a specially designed uniaxial tensile tester equipped with an optical train, laser micrometer and load cell. The system allows simultaneous determination of the mechanical (true stress, true strain) and optical (birefringence) properties of polymers during stretching at desired temperatures. The details of this on-line measurement system were reported earlier [45,46]. In this method white light is used as the light source to get the order number of retardation automatically. Birefringence is measured by the ratio of the real time retardation values to the real time thickness values measured at the same time and at the same location. This is accomplished using a laser micrometer mounted at an oblique angle that measures the width of the sample continuously at the symmetry midplane that remains stationary during the deformation process. This was accomplished through the built-in two crossheads that move in opposite directions. We then use the uniaxial symmetry (Eq. (1)) present in these materials to calculate the real time thickness (Eq. (2)) with the knowledge of initial thickness. The true stress is defined as the ratio of the tensile force to the actual cross section of the sample. In order to get the true stress (Eq. (5)), we directly measure tensile force by a load cell and divide it by the real time cross-sectional area of the film. The real time cross-sectional area of the film is the product of the width determined by the laser micrometer and the thickness (Eq. (2)). For elongation we define three parameters, i.e. stretch ratio, engineering strain and true strain. Stretch ratio is the ratio of the final length of the stretched sample to its initial length. Engineering strain is defined as the ratio of elongation (difference between the final length and the initial length) to the initial length of the sample. As for the true strain, we relate the state of elongation directly to the reduction in the local width of the sample. This is the same local mid region of the sample where the retardation measurements are made. We then combine the uniaxial symmetry (Eq. (2)) with the incompressibility assumption (Eq. (3)) and determine the true strain (Eq. (4)).

These relationships and the derivations are shown below.

$$W_t/W_o = D_t/D_o \tag{1}$$

$$D_t = \frac{W_t/W_o}{D_o} \tag{2}$$

$$D_o W_o L_o = D_t W_t L_t \tag{3}$$

In this research, we define the true strain and true stress as

$$\text{True strain} = \frac{\text{Elongation}}{\text{Initial length}} = \frac{L_t - L_o}{L_o} = \frac{\Delta L}{L_o} = \left(\frac{W_o}{W_t}\right)^2 - 1 \tag{4}$$

$$\text{True stress} = \frac{\text{Force}}{\text{Cross}-\text{sectional area}} = \frac{F_t}{W_t D_t} = \frac{F_t}{\left[\left(W_t^2/W_o\right)D_o\right]} \tag{5}$$

where W_t is the real time width of the film; W_o is initial width of the film; D_o is initial film thickness; D_t is real time film thickness; L_o is initial length of the film; L_t is real time length of the film; F_t is force.

The incompressibility assumption is reasonable for the PMMA and PHB-Cl blends since there is no crystallization taking place during stretching.

3. Results and discussion

3.1. Thermal analysis

Thermal transitions observed during DSC heating of pure PHB-Cl are shown in Fig. 1. The glass transition in PHB-Cl occurs between −10 and 10 °C. This is a wider interval than we reported for its unchlorinated counterpart, 0–4 °C [43]. Melting along with simultaneous degradation is also apparent at temperatures above 130 °C. In a previous publication we have shown that chlorination reduces the melting temperature of PHB-Cl from 175 to 148 °C along with its crystallinity [43].

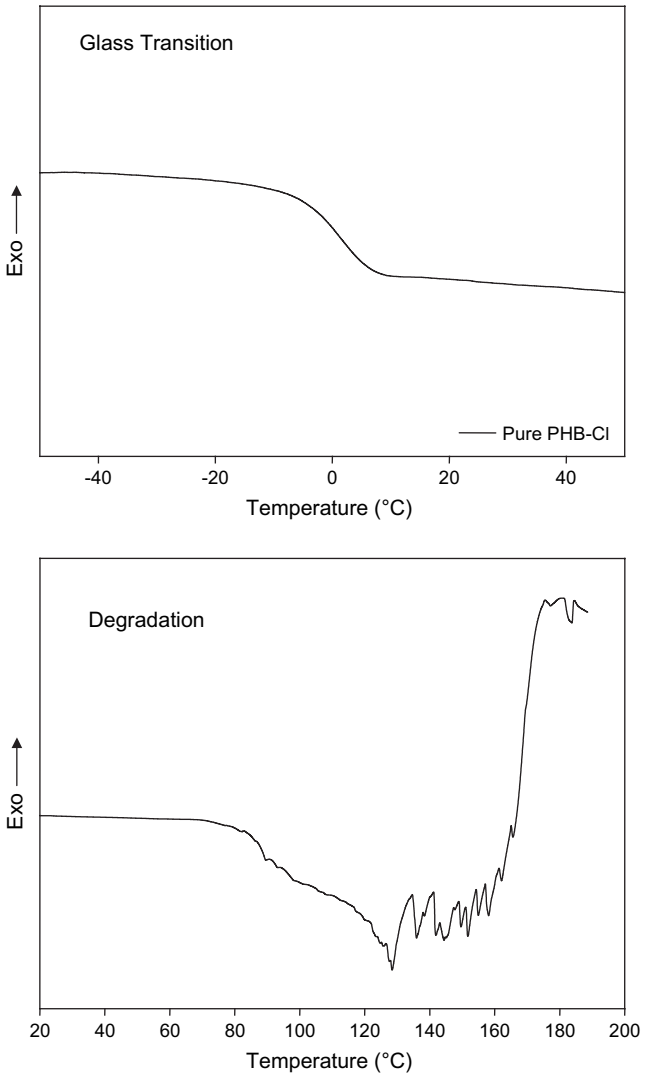

Fig. 1. Glass transition and degradation behavior of pure PHB-Cl.

Fig. 2 shows the glass transition behavior of PMMA with PHB-Cl addition. PHB-Cl reduces the glass transition temperature and widens the transition region. This is clearly evidenced in Fig. 2b and c from the first derivative of heat flow and the full width at maximum height values. Earlier, it was reported that the PHB (unchlorinated) and a-PMMA form a single glassy amorphous phase in compositions up to 20 wt% of PHB at room temperature. The broadening of the glass transition region by the addition of PHB-Cl indicates the development of micro-heterogeneities. These micro-scale composition fluctuations certainly account for a distribution in both the relaxation time and degree of cooperativity of segmental relaxation [47].

3.2. Mechano-optical behavior during uniaxial stretching

Temperature and composition effects on the mechano-optical behavior of uniaxially deformed PMMA/PHB-Cl blends will be discussed in the following sections.

3.2.1. Effect of temperature

Fig. 3 compares the true and engineering mechanical behavior of pure PMMA during uniaxial stretching to a stretch ratio of 3× (300%) at, below and above its T_g followed by 10 min holding stage at the processing temperature. Comparison of the stress values in the true and engineering data reveals that the stress levels are underestimated in the engineering data since the measured tensile force is divided by the initial cross-sectional area of the sample and the reduction in the cross-sectional area of the sample is not taken into account during stretching. In addition, the relaxation behavior in the true stress and true strain graph in Fig. 3 shows that even though the stretching globally comes to an end, the middle section of the sample where all measurements are made continues to deform as the strains in this section is independently measured by the built in laser micrometer that is monitoring the width of the sample continuously throughout the stretching and holding stages. This is not observable in the engineering data that relies on gage separation to determine the strains. The strain hardening is also much more apparent in the true mechanical data. The strain hardening is suppressed as the temperature is increased. Both engineering and true mechanical data show that the modulus increases as the temperature is decreased below the glass transition temperature.

In Fig. 4, birefringence behavior of pure PMMA is shown as a function of time (4a) and true strain (4b) during stretching. The birefringence levels are very small, in the order of 10^{-4}, typically observed for PMMA. The changing slope of the curves in Fig. 4a and b clearly evidences that the birefringence build up during stretching depends on the temperature of stretching as expected. The samples stretched at and below the glass transition temperature display strong negative birefringence ($n_{\|} < n_{\perp}$) initially and levels off with further stretching indicating that the chains are approaching their limit of extensibility at large strains. When PMMA films are stretched at temperatures above their T_g, on the other hand, birefringence remains unchanged close to zero throughout the stretching. Several factors could play a role for the birefringence levels to remain close to zero when stretched above the T_g. First of all, the chains, especially the ester side groups which are the main contributors to the polarizability anisotropy in PMMA, have enhanced degrees of freedom and assume several conformations above the T_g canceling out each other. The state of orientation of the main chain and its birefringence contribution is not critical since the polarizability anisotropy due to alpha-methyl group along the main chain of PMMA is very low [26,27,48]. In fact, slight positive birefringence in PMMA can only be achieved when it is stretched at very high temperatures above its T_g and cannot be frozen in on removal of the stress even with very fast cooling [49,50]. Another cause for the birefringence levels to remain around zero during stretching above the T_g is the thermal dissociation of the network junctions in PMMA. There is a common agreement in the literature that the ‘‘predominant’’ network association in PMMA is the dipole–dipole interactions between the ester side groups [29,51]. It has been proposed that increasing the temperature can dissociate these important cohesion points and influence

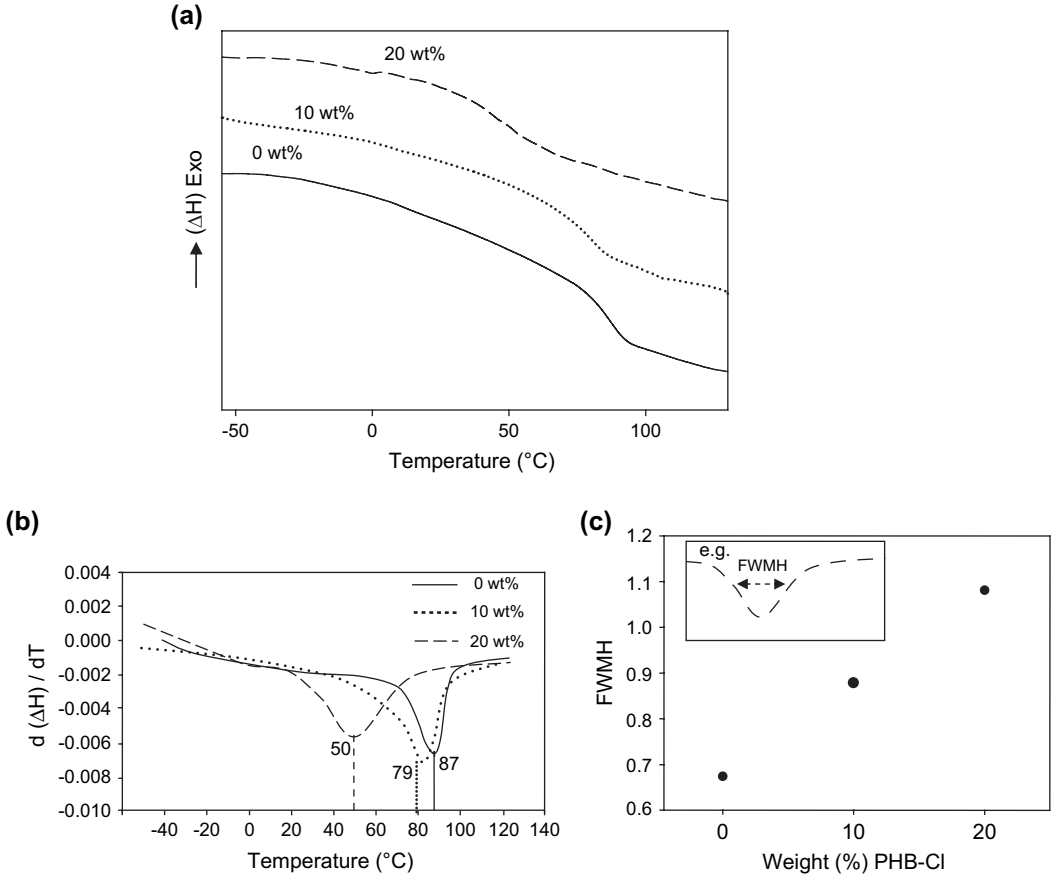

Fig. 2. (a) Glass transition curves of the PMMA/PHB-Cl blends; (b) first derivative of heat flow during glass transition; (c) full width at maximum height values of the graphs in 2b.

the deforming network and hence the birefringence levels. Above the T_g, these dipole associations get weaker due to enhanced thermal agitation between the side groups and reduce in number rendering a less connected network with less number of entanglements in a rubbery stage. This, in turn, favors the relaxation of the chains over orientation and hence negative birefringence cannot build up during stretching.

The linearity of the true strain rate versus true strain graph in Fig. 4c indicates that the sample experiences an affine deformation at all temperatures investigated near the T_g.

Fig. 5 shows birefringence–time and birefringence–true stress behavior for the stretching and the relaxation period. Above the glass transition temperature, birefringence remains unchanged close to zero throughout the stretching and the relaxation stage. At the glass transition temperature, birefringence decays to negative values upon stretching and remains at the same value unchanged throughout the relaxation period. Below the glass transition temperature, on the other hand, negative birefringence does not stay constant during relaxation but recovers to a certain extent, though not completely, along with

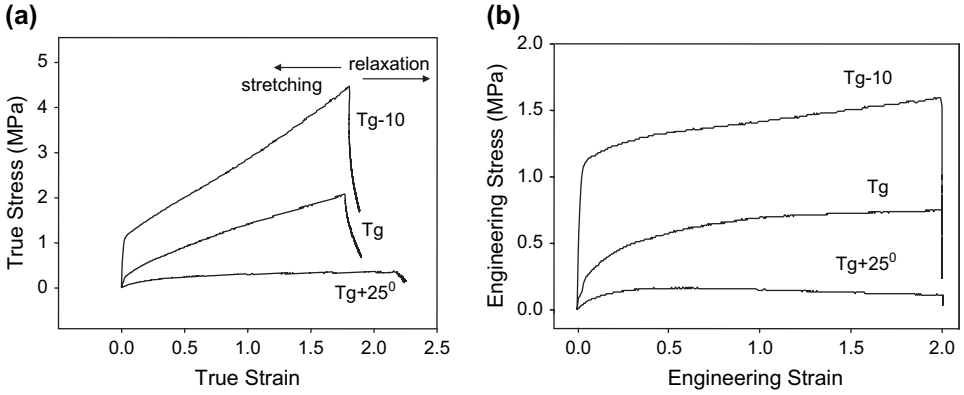

Fig. 3. Mechanical behavior (true and engineering) of pure PMMA during uniaxial stretching to a stretch ratio of 3× (or 300%) at, below and above its T_g followed by 10 min subsequent relaxation at the same temperature.

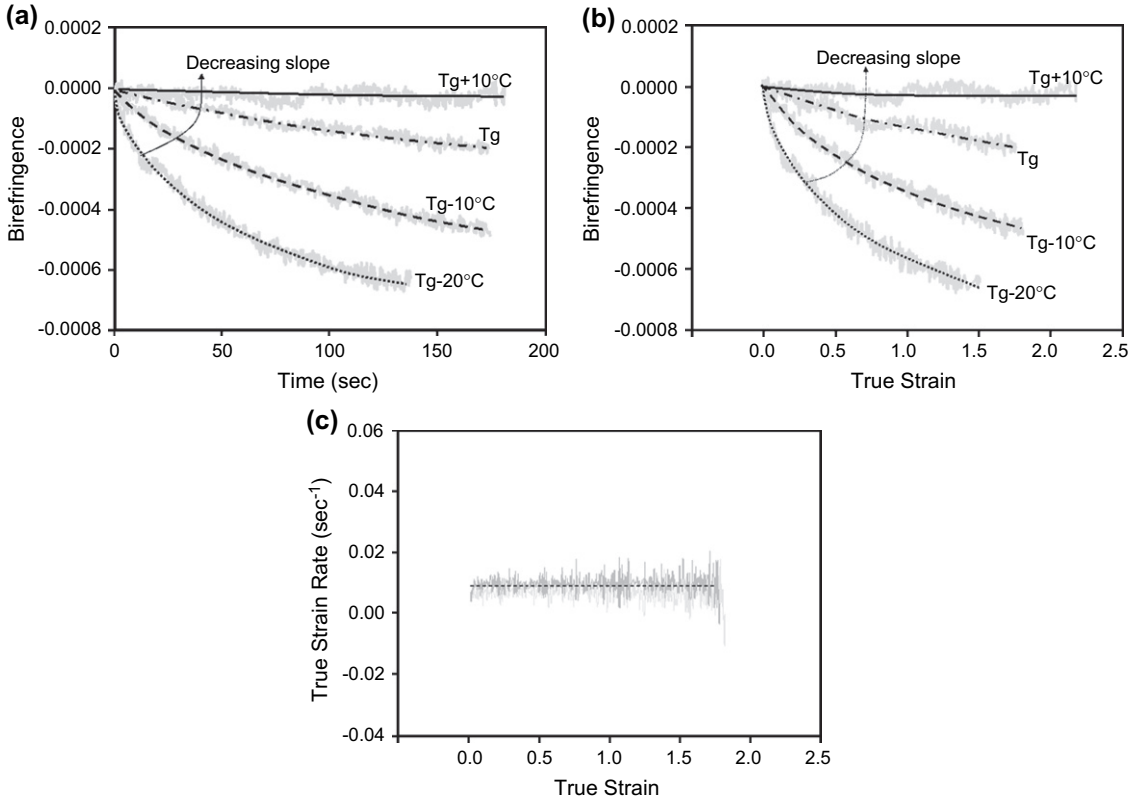

Fig. 4. Optical (birefringence) behavior of pure PMMA during uniaxial stretching to a stretch ratio of 3× (or 300%) at, below and above its T_g. (a) Birefringence–time; (b) birefringence–true strain; (c) true strain–true strain rate.

stress. It should be noted that birefringence relaxation occurs only for those samples stretched below the T_g where chain mobility is in fact lower. It has been proposed through theoretical studies [51] that stretching below the T_g results in dissociation and break up of the dipole–dipole cohesion points in PMMA network. The results of our relaxation experiments support this view. Strain-induced dissociation of these cohesion points render a less connected network with higher ability to relax during holding. It is also important to note that these results indirectly evidence the presence of the network associations proposed earlier.

The mechano-optical behavior during stretching and subsequent relaxation is shown for PMMA/PHB-Cl (90/10 wt%) blends in Fig. 6. The stretching was performed at 10 °C below,

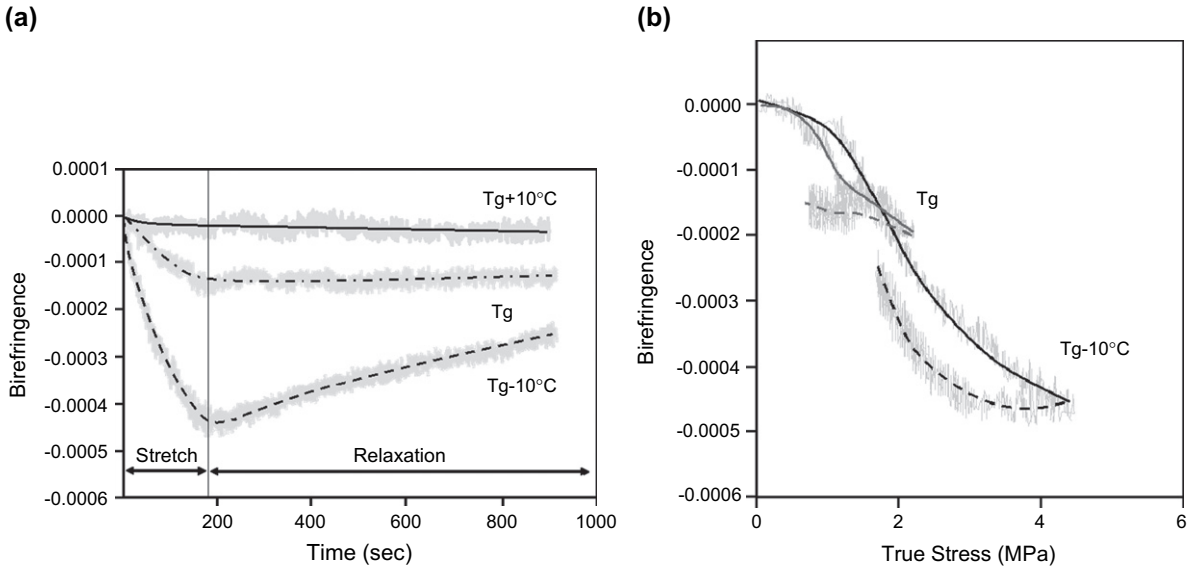

Fig. 5. Birefringence–time and birefringence–true stress behavior of pure PMMA during uniaxial stretching to a stretch ratio of 3× (or 300%) at, below and above its T_g followed by 10 min subsequent relaxation at the same temperature.

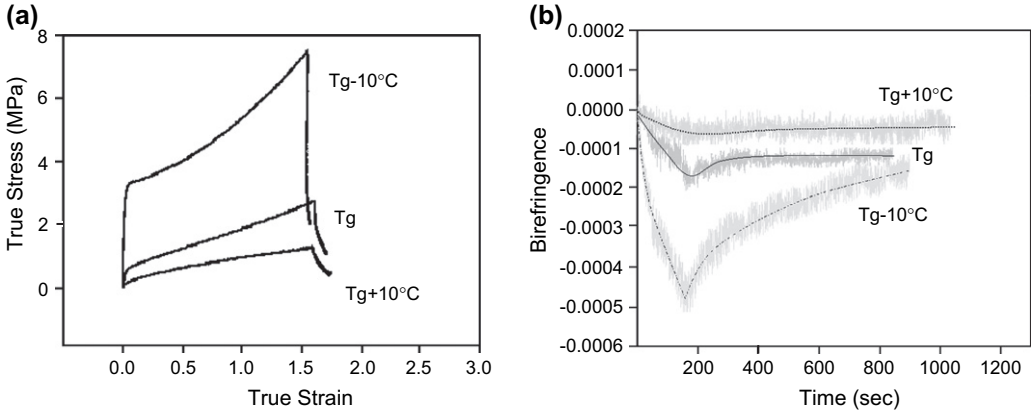

Fig. 6. True stress–true strain and birefringence–time graph for PMMA/PHB-Cl (90/10 wt%) blend.

10 °C above and at the glass transition temperature of the polymer blend. The behavior is very similar to that described for pure PMMA. The same is true for the PMMA/PHB-Cl (80/20) blend.

3.2.2. Composition effect

As we have presented earlier in Section 2.2, the glass transition behavior of pure PMMA changes appreciably when blended with biodegradable PHB-Cl. In the presence of PHB-Cl, T_g decreases and the glass transition takes place in a much broader temperature range, yet does not exhibit two distinct transition temperatures indicative of macro-phase separation.

In order to investigate the composition effect, we have first conducted stretching experiments at, below and above the corresponding glass transition temperature of each polymer system.

Fig. 7 shows true stress versus true strain data for three polymer systems at, below and above their corresponding T_g values. The blend systems exhibit higher modulus and higher stress values at all strain ranges during stretching. This effect is amplified as the amount of biodegradable PHB-Cl

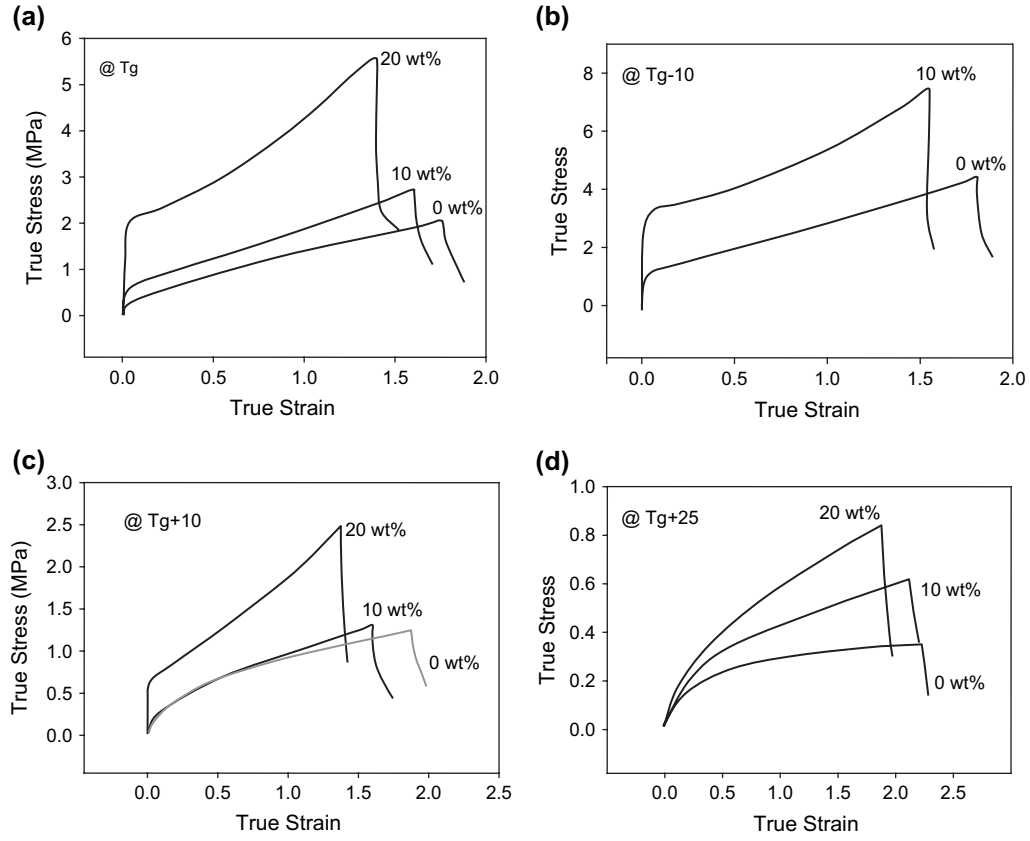

Fig. 7. True stress versus true strain behavior of three polymer systems at, below and above their corresponding T_g values.

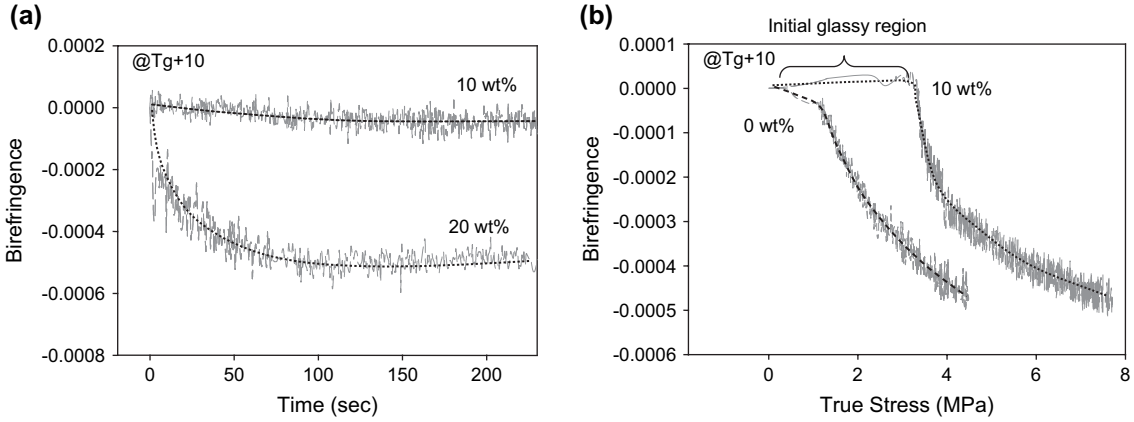

Fig. 8. Birefringence–time (left graph) and birefringence–true stress (right graph).

component is increased in the blend. At first glance, this result is somewhat counterintuitive since one would expect lower modulus and stress values in the blend systems due to their lower glass transition temperatures. Fig. 8 shows a similar counterintuitive behavior with the birefringence data. For instance, when stretched at $T_g + 10$ °C (Fig. 8a), the blend system with 20 wt% PHB-Cl exhibits considerably higher negative birefringence than the blend system with 10 wt% PHB-Cl. Similarly in Fig. 8b, the blend system with 10 wt% PHB-Cl shows a much larger initial glassy region than that of pure PMMA when stretched at $T_g - 10$ °C.

We attribute the origin of this counterintuitive behavior to the broadening of the glass transition region. Due to the broadening, the molecular mobility of the three polymer systems is not comparable when stretched at their corresponding glass transition values or a specific degree below or above it. This is depicted in Fig. 9 by comparing the shaded areas under the derivative curve of the heat flow considering the case of $T_g + 10$ °C. The shaded area increases as the PHB-Cl content is increased. This indicates for the blend systems that there is still a fair amount of molecular chains that are still within the transition region and not entirely softened. Therefore, the

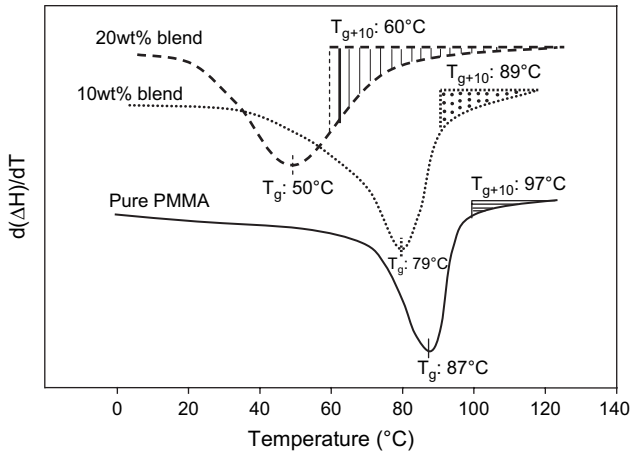

Fig. 9. Derivative of glass transition temperature versus temperature for the three systems.

blend systems, in spite of their lower glass transition values, exhibit a more glassy behavior than the pure PMMA when stretched at their corresponding T_g values or a certain degree above or below it.

We have also investigated the blend effect at one selected stretching temperature, 75 °C. At this temperature, the blend system with 20 wt% PHB-Cl is well above its glass transition temperature whereas the blend system with 10 wt% PHB-Cl is within its glass transition temperature. Pure PMMA, on the other hand, is below its glass transition temperature at 75 °C. Although the three polymer systems are not in a comparable stage of molecular mobility at this single selected temperature, these experiments were useful to show that PHB-Cl in fact acts as a plasticizer for PMMA. Plasticizing effect and enhanced relaxation of the blends with PHB-Cl could be attributed to the enlargement of the free volume in the micro-heterogeneous blends and hence improved mobility by the addition of PHB-Cl. This was evidenced by the broadening of the T_g. PHB-Cl could also act so as to prevent some of the dipole–dipole associations of PMMA that would yield a less connected network structure leading to enhanced relaxation for the blends.

The true stress and true strain data for the three polymer systems are shown in Fig. 10 for the selected temperature of 75 °C. Clearly, at this temperature, the blend systems with the higher amount of PHB-Cl exhibit lower modulus and stress levels during stretching due to their higher molecular mobility at this temperature.

Fig. 11 shows that the addition of PHB-Cl to the PMMA shifts the birefringence levels closer to zero values during stretching at 75 °C. Birefringence versus time and birefringence versus true strain behavior in Fig. 11 are very similar to each other for all the blend compositions. This indicates that addition of PHB-Cl to the PMMA did not influence the affine deformation behavior. When the PHB-Cl concentration reaches 20%, a slight positive birefringence development is observed from the very start of the stretching. This is quite evident in Fig. 12 as the negative stress optical behavior crosses over to positive stress optical behavior in between 10 and 20 wt% PHB-Cl concentrations. As shown in Fig. 13, zero crossing occurs at 18 wt% PHB-Cl at 75 °C.

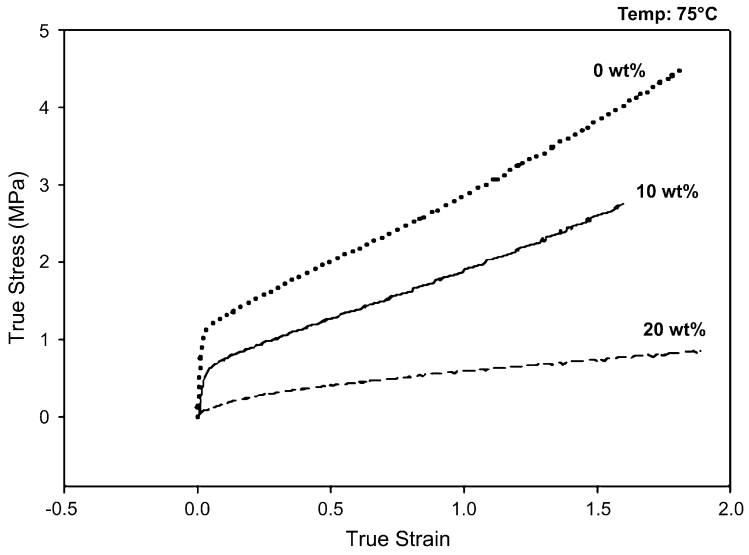

Fig. 10. True stress and true strain behavior at different blend ratios.

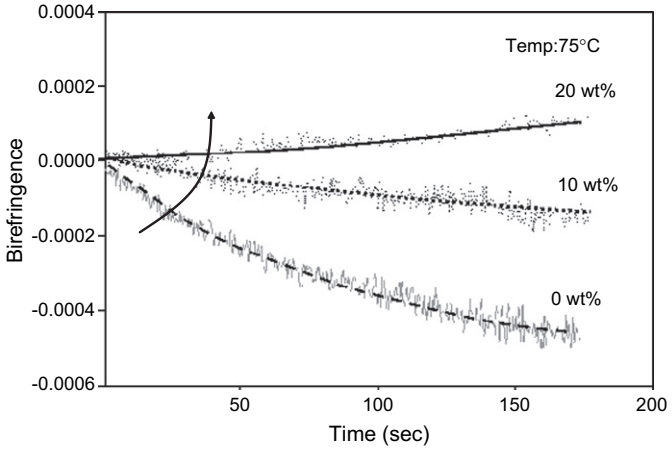

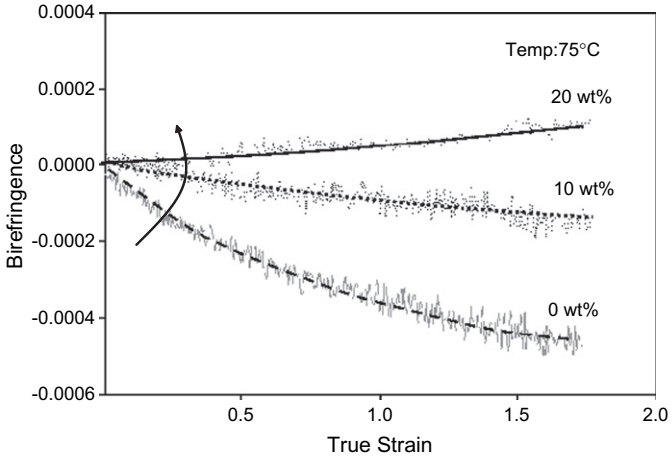

Fig. 11. Birefringence–time and birefringence–true strain at different blend ratios.

During relaxation, as shown in Fig. 14, the negative birefringence levels developed during stretching recover to some degree in the pure PMMA. In the 10% blend system, the birefringence level recovers slightly and levels off at a value close

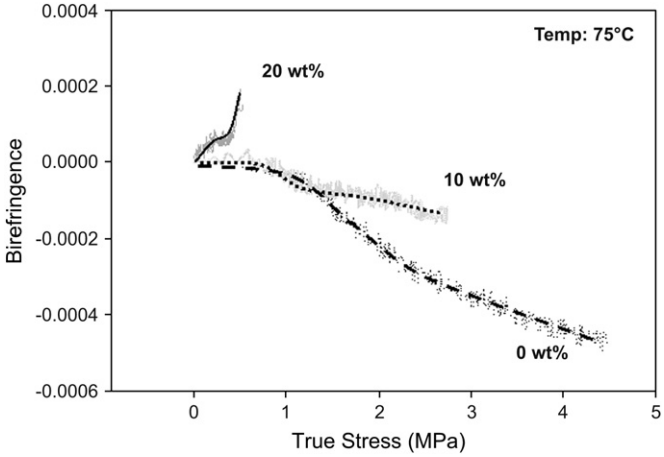

Fig. 12. Birefringence–true stress behavior at different blend ratios.

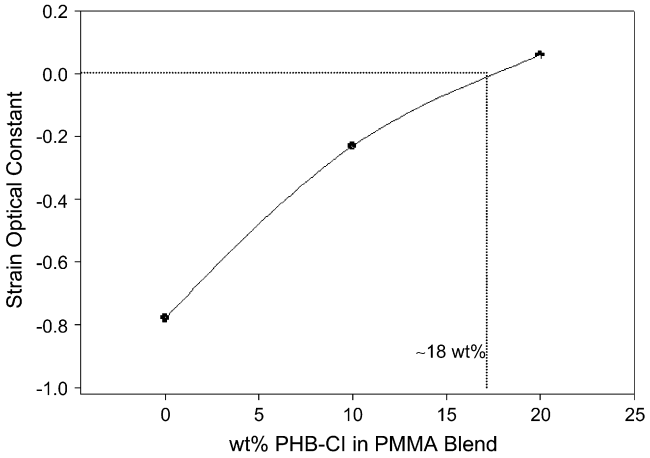

Fig. 13. Ideal composition range for the blend to exhibit zero birefringence.

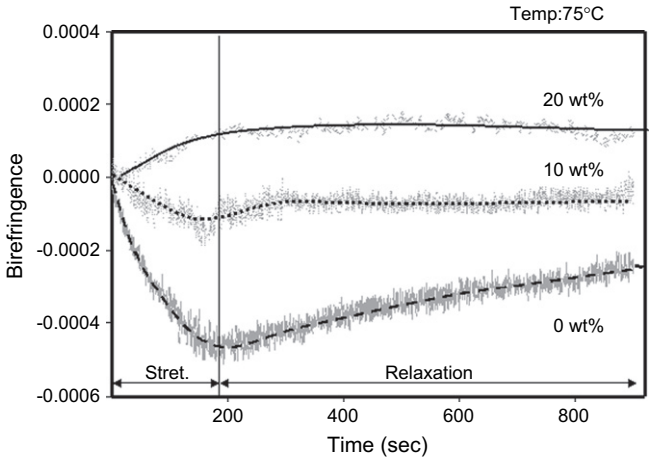

Fig. 14. Relaxation behaviors of the blends.

to zero. The blend system with 20 wt% PHB-Cl displays positive birefringence upon stretching and subsequent relaxation does not change the birefringence values.

The WAXD patterns of the stretched films of 90/10 blend and the pure PMMA are shown in Fig. 15.

At these blend ratios no crystallinity is observed in spite of the semi-crystalline nature of the PHB-Cl polymer in its unblended form. In a previous publication, we have shown that the chlorine content decreases the crystallinity [43]. Since the presence of crystallinity adversely affects the optical clarity of the films, the PHB content in the blends should be kept below 20% for optical applications.

In these binary blends, PHB-Cl acts like a plasticizer in the PMMA blend. Consequently, it also influences the network cohesion points, i.e. dipolar associations in the ester side groups, of PMMA during stretching and hence the birefringence

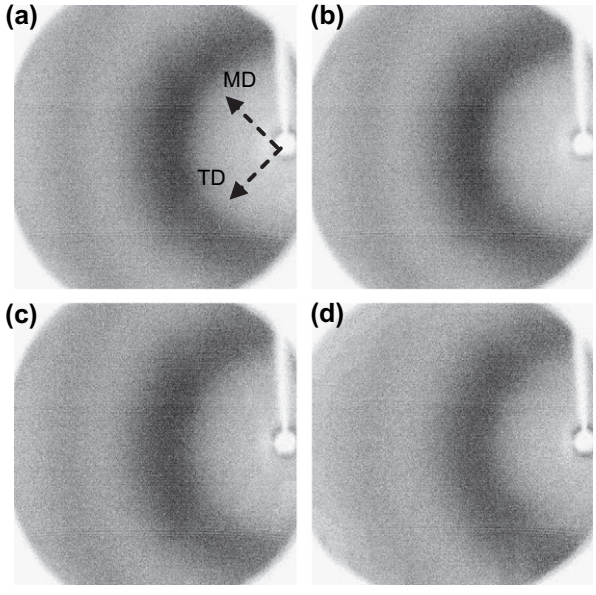

Fig. 15. WAXD pictures of the amorphous halos. All samples are stretched to 3×. (a) Pure PMMA at $T_g - 10$; (b) pure PMMA at T_g; (c) PMMA/PHB-Cl (90/10) at $T_g - 10$; (d) PMMA/PHB-Cl (90/10) at T_g.

levels. The polar nature of the PHB-Cl molecule could also act so as to dissociate some of the dipolar ester associations in PMMA and bring the birefringence levels closer to zero. In addition, the stress optical behavior becomes positive at 20 wt% PHB-Cl loading suggesting that there is a positive contribution of PHB-Cl to the intrinsic birefringence of the blend.

The decomposition behavior of the PHB-Cl in the blend polymer has not been covered in this paper. Further investigation is necessary to determine if PHB-Cl component could actually be reached by the bacteria as they may be impeded by the presence of surrounding PMMA chains.

4. Conclusions

We have successfully synthesized PHB-Cl and blended them for the first time with commercial atactic PMMA and prepared films via solution casting. These blends are shown to be partially miscible. The large deformation mechano-optical analysis indicates that the blend compositions containing about 18 wt% of PHB-Cl exhibit zero in-plane birefringence to large deformation levels. The zero birefringence in the blend films is made possible at the expense of decreasing the glass transition of the materials to some extent by the presence of PHB-Cl in the blends.

By judicious composition selection the blends can also be used to develop films with negative or positive in-plane retardation by appropriate stretching method. This makes these blends suitable for optical retarder films used in LC displays as well.

Acknowledgements

This material is based upon work supported by the National Science Foundation under International Grant No. 9974598.

References

[1] Doi Y. Microbial polyesters. New York: VCH Publishers; 1990.
[2] Anderson AJ, Dawes EA. Microbiol Rev 1990;54:450.
[3] Brandl H, Gross RA, Lenz RW, Fuller RC. Adv Biochem Eng/Biotechnol 1990;41:77.
[4] Hocking PJ, Marchessault RH. In: Griffing GJL, editor. Biodegradable polymer. London: Blake Academic and Professional; 1994.
[5] Steinbüchel A, Valentin HE. FEMS Microbiol Lett 1995;128:219.
[6] Hazer B, Lenz RW, Fuller RC. Polymer 1996;37:5951.
[7] Curley JM, Hazer B, Lenz RW, Fuller RC. Macromolecules 1996; 29:1762.
[8] Kim YB, Lenz RW, Fuller RC. Macromolecules 1992;25:1852.
[9] Hazer B, Torul O, Borcakli M, Lenz RW, Fuller RC, Goodwin SD. J Environ Polym Degrad 1998;6:109.
[10] Hoffman A, Kreuzberger S, Hinrichsen G. Polym Bull 1994;33:355.
[11] Grassie N, Murray EJ, Holmes PA. Polym Degrad Stab 1984;6:95.
[12] Cavalloro P, Immirzi B, Malinconico M, Martuscelli E. Macromol Rapid Commun 1994;15:103.
[13] Kowalczuk M, Adams G, Jedlinski Z. Macromolecules 1994;27:572.
[14] Doi Y, Kitamura S, Abe H. Macromolecules 1995;28:4822.
[15] Avella M, Martuscelli E. Polymer 1988;29:1731.
[16] Greco P, Martuscelli E. Polymer 1989;30:1475.
[17] Dubini Paglia E, Beltrame PL, Canetti M, Seves A, Mercandalli B, Martuscelli E. Polymer 1993;34:996.

[18] Sadocco P, Canetti M, Seves A, Martuscelli E. Polymer 1993;34:3369.
[19] Canetti M, Sadocco P, Siciliano A, Seves A. Polymer 1994;35:2884.
[20] Lotti N, Pizzoli M, Ceccorulli G, Scandola M. Polymer 1993;34:4935.
[21] Siciliano A, Seves A, De Marco T, Cimmino S, Martuscelli E, Silvestre C. Macromolecules 1995;28:8065.
[22] Cimmino S, Iodice P, Silvestre C. Thermochim Acta 1998;321:89.
[23] Avella M, Errico ME, Immirzi B, Malinconico M, Falcigno L, Paolillo L. Macromol Chem Phys 1998;199:1901.
[24] Lee J, Nakajima K, Ikehara T, Nishi T. J Polym Sci Part B Polym Phys 1997;35:2645.
[25] El-Hadi A, Schnabel R, Straube E, Müller G, Riemschneider M. Macromol Mater Eng 2002;287:363–72.
[26] Andrews RD, Hammack TJ. J Polym Sci Part C 1964;5:101–12.
[27] Trapeznikova ON, Zhurina MN. J Phys Chem (USSR) 1950;24:1471.
[28] Kolsky H, Shearman AC. Proc Phys Soc 1943;55:383.
[29] Hammack TJ, Andrews RD. J Appl Phys 1965;36:3574–81.
[30] Kashiwagi M, Folkes MJ, Ward IM. Polymer 1971;12:697.
[31] Purvis J, Bower DI. Polymer 1974;15:645.
[32] Saito H, Inoue T. J Polym Sci 1987;25:1629–36.
[33] Ramesh S, Yahaya AH, Arof AK. Solid State Ionics 2002;148:483–6.
[34] Hahn BR, Wendorff JH. Polymer 1985;26:1619.
[35] Liau WB, Chang CF. J Appl Polym Sci 2000;76:1627–36.
[36] Iwata S, Tsukahara H, Nihei E, Koike Y. Jpn J Appl Phys 1996;35:3896.
[37] Iwata S, Tsukahara H, Nihei E, Koike Y. Appl Opt 1997;36:4549.
[38] Tagaya A, Iwata S, Kawanami E, Tsukahara H, Koike Y. Jpn J Appl Phys 2001;40:3677.
[39] Tagaya A, Iwata S, Kawanami E, Tsukahara H, Koike Y. Jpn J Appl Phys 2001;40:6117.
[40] Tagaya A, Ohkita H, Mukoh M, Sakaguchi R, Koike Y. Science 2003;301:812–4.
[41] Koçer H, Borcaklı M, Demirel S, Hazer B. Turk J Chem 2003;27:365.
[42] Hazer B, Lenz RW, Fuller RC. Macromolecules 1994;27:45.
[43] Arkin AH, Hazer B, Borcakli M. Macromolecules 2000;33:3219.
[44] Arkin AH, Hazer B. Biomacromolecules 2002;3(6):1327–35.
[45] Koike Y, Cakmak M. Polymer 2003;44:4249–60.
[46] Beekmans F, Posthuma de Boer A. Macromolecules 1996;29:8726–33.
[47] Schneide HA, Cantow HJ, Wendland C, Leikauf B. Makromol Chem 1990;191:2377–86.
[48] Reed BE. J Polym Sci (C) 1967;16:1887.
[49] Trapeznikova ON, Zhurina MN. Zh Fiz Khim 1950;14:1471.
[50] Peukert H. Kautsch Gummi Kunstst 1951;41:154.
[51] Raha S, Bowden PB. Polymer 1972;13(4):174–83.